Indoor Range-Direction-Movement SAR for Drone-based Radar Systems

Jiaming Yan[#1], Zhengyu Peng[#2], Hong Hong[#1], Xiaohua Zhu[#1], Qi Lu[#3], Beibei Ren[#3], Changzhi Li[#2]
[#1] *School of Electronic and Optical Engineering, Nanjing University of Science and Technology*
Nanjing, Jiangsu 210094, China
[1]benjaminyan2494@163.com
[1]hongnju@njust.edu.cn
[1]zxh@njust.edu.cn
[#2] *Department of Electrical and Computer Engineering, Texas Tech University*
Lubbock, TX 79409, USA
[2]zhengyu.peng@ttu.edu
[2]changzhi.li@ttu.edu
[#3] *Department of Mechanical Engineering, Texas Tech University*
Lubbock, TX 79409, USA
[3]qi.lu@ttu.edu
[3]beibei.ren@ttu.edu

***Abstract*—Locating a target close to a wall or a corner is a challenge for indoor synthetic aperture radar (SAR) imaging because the radar does not have enough space to effectively form a large aperture. In this paper, we propose a range-direction-movement method for a drone-based frequency-modulated continuous-wave (FMCW) radar system. The solution can effectively form a large aperture when the antennas move in range direction instead of azimuth. Experiments have been conducted to demonstrate the accuracy and robustness of the proposed method.**

Keywords—SAR; FMCW radar; drone; indoor.

I. INTRODUCTION

Synthetic aperture radar (SAR) uses azimuth movement of a radar antenna over a target region to achieve finer spatial resolution than conventional beam-scanning radars. Frequency-modulated continuous-wave (FMCW) SAR leads to compact, lightweight, and low-cost high-resolution imaging systems. As a result, FMCW SAR systems are playing an important role in airborne earth observation and regional imaging [1]-[4], demonstrating great potential for civil and military applications.

To implement a high-resolution SAR system, a moving platform that carries the radar is necessary. Benefiting from the rapid advancement of drone technologies [5]-[6] as well as the lightweight of modern portable FMCW radar system based on integrated semiconductor technologies, it becomes possible to implement an FMCW SAR system on an operational drone. For example, [7] developed an inexpensive method to produce high resolution digital elevation model using a DJI drone and an InSAR system. [8] presented a processing algorithm able to acquire high-resolution airborne SAR data. In [9], a low-cost SAR imaging system based on a small consumer drone that can be controlled through a Wi-Fi connection was reported. In [10], the drone payload when carrying an L-band FMCW SAR system was studied.

The above works were all implemented in outdoor environment, where the high resolution in the azimuth direction was achieved by coherently processing the Doppler modulated returns as the antenna scans across a large synthesized aperture. However, due to the limited space of the indoor environment, if targets are close to a wall or a corner, the drone cannot fly too close in the azimuth direction, making it difficult for conventional squint SAR imaging method to form a large effective aperture. Without enough height, it is challenging for squint SAR method to efficiently cover the entire room. Therefore, developing a method to focus on a region that is close to a wall is necessary for indoor SAR imaging applications.

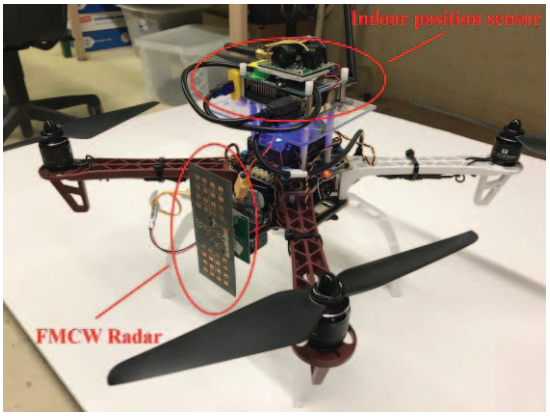

Fig. 1. The drone-based radar system.

This paper proposes a range-direction-movement technique based on wavenumber domain algorithm [11]. The proposed method can form a large aperture when the antennas move in the range direction instead of the azimuth. Carried by an operational drone, the radar can focus on a region close to a wall or a corner and obtain high-resolution SAR images.

This paper is organized as follows. Section 2 presents the drone-based FMCW radar system. In Section 3, the theory of the range-direction-movement SAR is detailed, and experimental results are described in Section 4. Finally, a conclusion is drawn in Section 5.

Fig. 2. Block diagram of range-direction-movement SAR algorithm.

II. Drone-based Radar System

The drone-based radar system is shown in Fig. 1, which consists of an FMCW radar, two antennas and a drone with an indoor position sensor.

A. FMCW radar system

The radar system is integrated on a Rogers RT/duroid 5880 flexible microwave substrate consisting of a flexible radio frequency (RF) board and a rigid baseband board. The bandwidth of the transmitted signal is 450 MHz and the center frequency is 24 GHz. The transmitted average power is around 8 dBm. Two 4×4 patch arrays are used to transmit and receive signals respectively. The beam width of each array is around 16.5°. In the receiver channel, the received signal is amplified by two low noise amplifiers (LNAs) and then mixed with the LO signal in a six-port structure. The six-port output circuit is amplified by differential baseband amplifiers and the receiver RF gain is around 34 dB. The baseband signal is digitized with 192 KHz sampling rate and 16-bit resolution for the real-time signal processing.

B. Drone

The experimental platform is a custom-built quadrotor. The main flight control is achieved by a Pixhawk flight controller. A companion computer Odroid XU4 is integrated to handle the sensor data and height control. A TeraRanger One distance sensor is added to measure height. The height controller runs with an Odroid XU4 with the update rate of 100 Hz. The horizontal positions of the quadrotor are controlled by a pilot using a Spektrum DX8 transmitter. An indoor GPS system from the Marvelmind Robotics is used to record the quadrotor horizontal positions.

III. Processing Method

In this section, we propose a range-direction-movement SAR imaging algorithm. A general block diagram of the method is shown in Fig. 2. The steps to implement the method are described below:

A. Flight path correction

Since the horizontal positions of the drone is manually controlled, the deviation of the drone's actual trajectory from the desired trajectory will be up to tens of centimeters. In the indoor environment, when the drone is flying close to a wall, the imaging region is close to the radar, so these errors cannot be ignored.

As shown in Fig. 3, the blue curve from A to B is the measured path of the drone, which can be tracked from the indoor GPS system. The coordinate at time t can be written as $(X(t), Y(t), H(t))$, where $t \in [0, T]$ with T being the duration of the flight; $X(t)$ and $Y(t)$ are the horizontal and vertical coordinates and $H(t)$ is the height of the drone, respectively. The red line AB is the desired path for the drone to fly. Using $Y(t)$ as the reference to align the two curves, the desired coordinate at vertical distance $Y(t)$ can be defined as

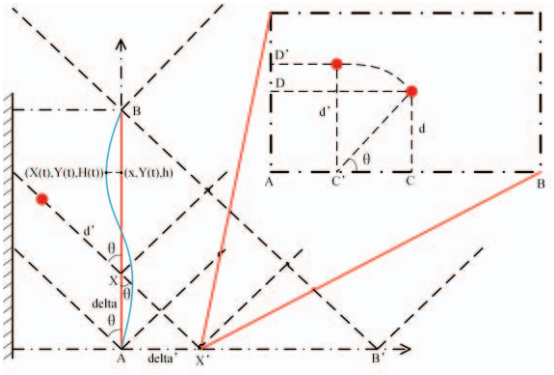

Fig. 3. Diagram illustrating the range-direction-movement SAR.

$(x, Y(t), h)$, where $t \in [0, T]$; x is the desired horizontal coordinate and h is the desired height set by the drone.

The FMCW raw data can be described by $f(\mathrm{s}_t)$, where s_t is the matrix of slow-time t received by the radar. $f(\mathrm{s}_t)$ is first transformed along the fast-time to obtain the time-range domain signal $\mathrm{F}(\mathrm{r}_t)$ by Fast Fourier transform (FFT), where r_t is the range matrix at slow-time t and has M points. The corrected range $\mathrm{r'}_t$ in the vertical coordinate $Y(t)$ can be calculated as:

$$\mathrm{r'}_t = \frac{X(t)-x}{|X(t)-x|}\sqrt{(X(t)-x)^2 + (H(t)-h)^2} \tag{1}$$

and the relationship between r_t and $\mathrm{r'}_t$ can be described as:

$$|\mathrm{r'}_t| = \mathrm{r}_t(m),\ m \in [1, M] \tag{2}$$

Thus at slow-time t, the actual range signal R_t is given by:

$$\mathrm{R}_t = \begin{cases} [0,0,\dots,0,\mathrm{r}_t(m),\mathrm{r}_t(m+1),\dots,\mathrm{r}_t(M)], & \mathrm{r'}_t < 0 \\ \mathrm{r}_t, & \mathrm{r'}_t = 0 \\ [\mathrm{r}_t(m),\mathrm{r}_t(m+1),\dots,\mathrm{r}_t(M),0,0,\dots,0], & \mathrm{r'}_t > 0 \end{cases} \tag{3}$$

where the total number of 0's is $(m-1)$ in each function. Finally, using IFFT to transform the modified time-range domain signal $\mathrm{F}(\mathrm{R}_t)$ back to the slow-time fast-time domain, the corrected data $f_0(\mathrm{s}_t)$ can be obtained.

B. Wavenumber domain algorithm(WDA)

The WDA is a conventional SAR focusing algorithm that can focus FMCW SAR data well in the broadside for high-squint cases [11]. The basic steps of the WDA are described below. First, the residual video phase (RVP) introduced by the applied dechirp-on-receive operation is removed. Then FFT is applied in the slow-time direction, and Stolt interpolation [1] is used to eliminate the range and azimuth coupling. Finally, two-dimensional IFFT is used to obtain the SAR image.

In our method, the WDA is used to accumulate the range-direction-modified raw data $f_0(\mathrm{s}_t)$ in the direction of the azimuth. Then a SAR image $S_{i,j}$ consists of $N = i \times j$ pixels is obtained with coordinates $(C'(i), D'(j))$ and amplitudes $A_{i,j}$, where $C'(i)$ and $D'(j)$ are the actual cross-range and downrange distance of the pixel $S_{i,j}$ in the WDA result.

C. Axis conversion

In indoor environment, when the drone flies in the range direction along the wall, the SAR image is not the real location of the region. The image needs to be converted with an angle θ,

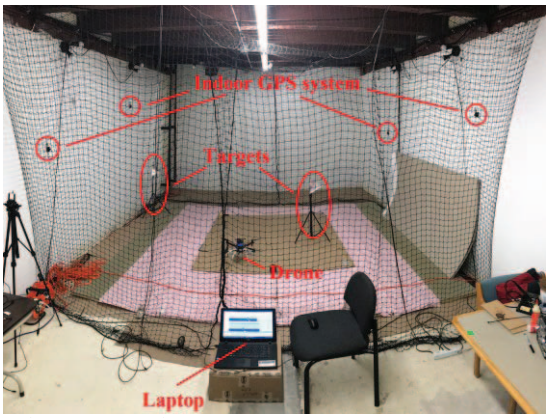

Fig. 4. Indoor SAR experiment setup.

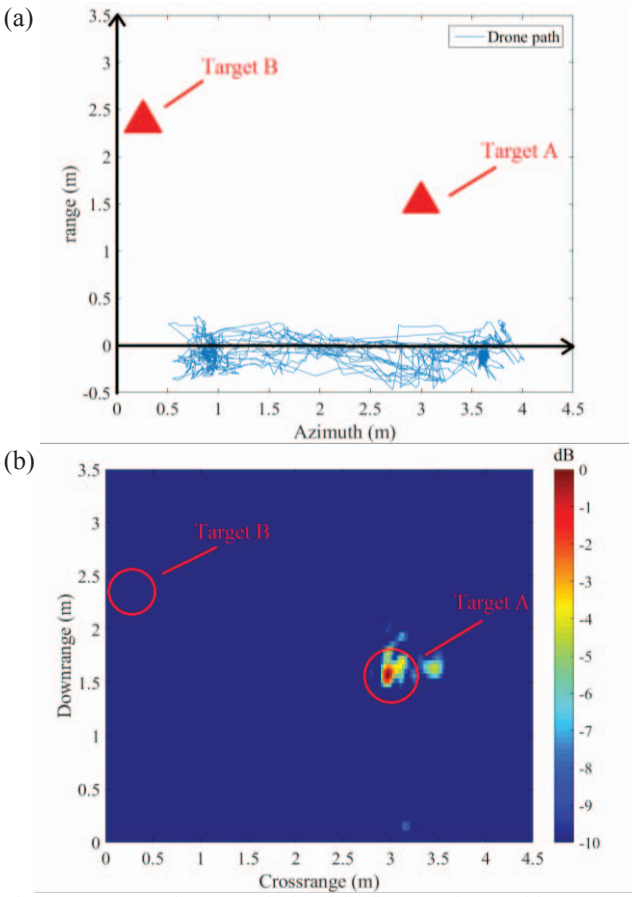

Fig. 5. Setup (a) and SAR result (b) of the first experiment with two targets using the WDA method.

which is half the beam-width of the antenna. The conversion is also illustrated in Fig. 3. The relationship between $(C'(i), D'(j))$ and $\big(C(i), D(j)\big)$ can be described as:

$$C(i) = C'(i) + D'(j) * cos\theta \tag{4}$$

$$D(j) = D'(j) - D'(j) * sin\theta \tag{5}$$

where $(C(i), D(j))$ is the actual cross-range and downrange locations of the pixel $S_{i,j}$. By doing this step to all the N pixels in the SAR image obtained from the WDA, we can obtain the actual SAR image of the region.

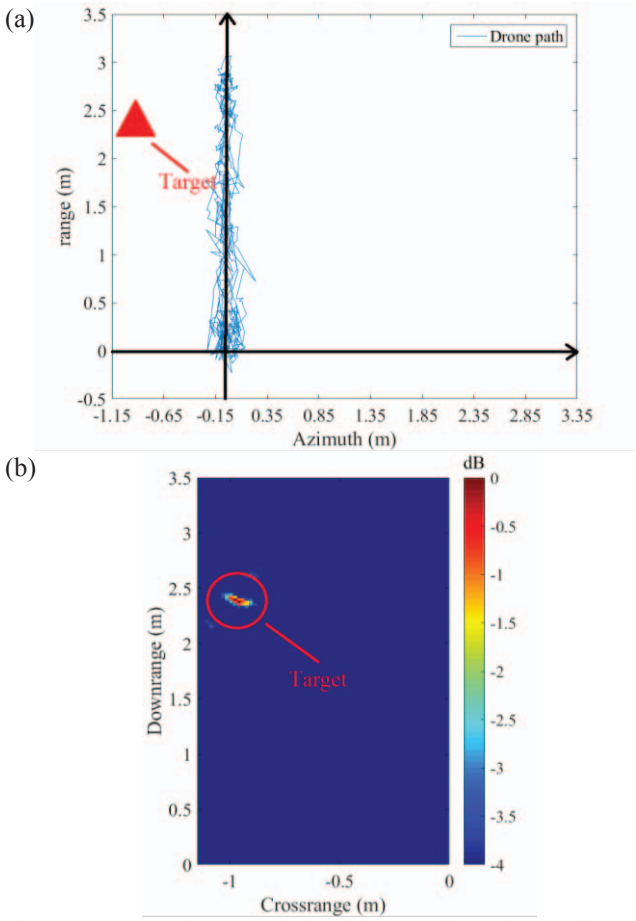

Fig. 6. Setup (a) and SAR result (b) of the second experiment with a single target using the proposed algorithm.

IV. Experimental Results

For calibration and testing, based on the range-direction-movement method, we designed three different experiments to focus on different indoor regions. The scene is shown in Fig. 4. The size of the indoor experiment zone was 4.5 m × 3.5 m. 4 position sensors was set to record the horizontal positions of the drone in real time and the desired height h of drone was set to 0.8-m.

A. Two targets with WDA method

The first set of images was obtained by the conventional squint SAR method with the drone flying in the azimuth direction only. A diagram illustrating the drone path and setup is shown in Fig. 5(a). The drone moved along a 4-m apertures. The two targets remained stationary while the drone was flying. The coordinates of target A and target B are (3m, 1.5m, 0.74m) and (0.25m, 2.4m, 0.83m), respectively.

The SAR result is illustrated in Fig. 5(b). In this experiment, the trajectory of the drone did not form an aperture large enough to focus on target B, which was close to the wall. As a result, the conventional squint SAR method was able to effectively "see" target A, but could hardly find target B. Therefore, the proposed range-direction-movement algorithm was used to solve the challenge.

(a)

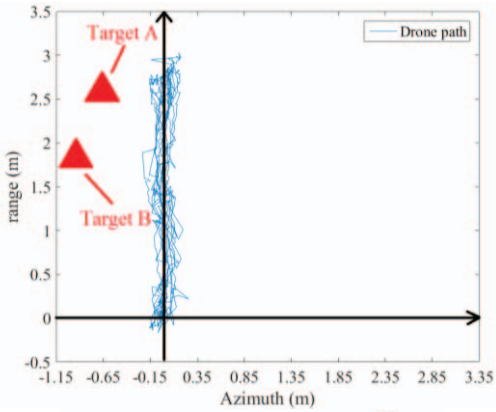

(b)

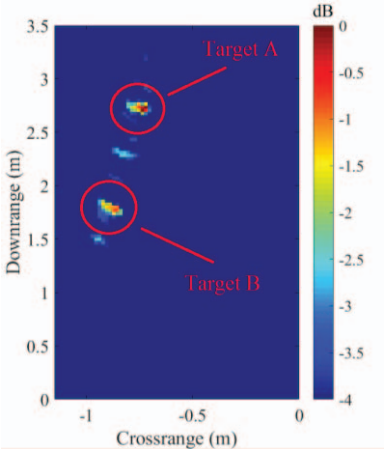

Fig. 7. Setup (a) and SAR result (b) of the third experiment with two targets using the proposed algorithm.

B. One target with range-direction-movement algorithm

To demonstrate the effectiveness of our algorithm, another experiment was performed with one target located at (-0.9m, 2.4m, 0.83m), which is the same location as target B in Section IV-A. The radar moved along the range direction by flying the drone for 2.8-m with a safe distance of 1.15-m from the wall. The drone path and setup are shown in Fig. 6(a).

The SAR result is illustrated in Fig. 6(b). From the picture, although the target is close to the wall, we can see it is well focused with a -4dB intensity scale. However, the result exhibited some downrange smearing. This is because the drone moved with a variable speed but the current algorithm does not perform speed correction, which will be addressed in the future works.

C. Two targets with range-direction-movement algorithm

To further demonstrate the high-resolution of our method, the third experiment was performed with two targets placed near a wall and a corner. In this experiment, the drone flew with a smoothly movement along the same measurement path as Section IV-B, and the setup is shown in Fig. 7(a). The coordinates of target A and target B are (-0.65m, 2.6m, 0.83m) and (-0.9m, 1.8m, 0.74m), respectively.

Fig. 7(b). shows the axis conversion results. The two targets can be clearly identified at the correct locations with a -4dB intensity scale. This experiment demonstrated that our method has the ability to image a region close to a wall with a high resolution.

V. Conclusion

This paper has proposed and validated a range-direction-movement technique based on the wavenumber domain algorithm to focus the indoor region close to a wall or a corner. The method accumulates a large aperture in range-direction-movement instead of azimuth direction, which is distinguished from conventional squint SAR methods. It enables a radar platform to obtain high-resolution image of near-wall and corner regions when it moves along the wall. The proposed solution is especially helpful in reducing the imaging time, as no extra movement of a drone is needed to form special apertures to cover those regions.

VI. Acknowledgments

This work was supported in part by the National Science Foundation (NSF) under Grant ECCS-1254838, the National Natural Science Foundation of China under Grant 81601568, the National Key Technology Support Program under Grant 2015BAI02B04, the NSF of Jiangsu Province under Grant SBK2014043201, and the Fundamental Research Funds for the Central Universities under Grant 30917011316.

References

[1] Wang R, Loffeld O, Nies H, et al. “Focus FMCW SAR data using the wavenumber domain algorithm”. IEEE Transactions on Geoscience and Remote Sensing, 2010, 48(4): 2109-2118.

[2] Gu C, Chang W, Li X, et al. “A New Distortion Correction Method for FMCW SAR Real-Time Imaging”. IEEE Geoscience and Remote Sensing Letters, 2017, 14(3): 429-433.

[3] Ribalta A. “Time-domain reconstruction algorithms for FMCW-SAR”. IEEE Geoscience and Remote Sensing Letters, 2011, 8(3): 396-400.

[4] Meta A, Hoogeboom P, Ligthart L P. “Signal processing for FMCW SAR”. IEEE Transactions on Geoscience and Remote Sensing, 2007, 45(11): 3519-3532.

[5] Wang W Q, Peng Q, Cai J. “Waveform-diversity-based millimeter-wave UAV SAR remote sensing”. IEEE Transactions on Geoscience and Remote Sensing, 2009, 47(3): 691-700..

[6] Xing M, Jiang X, Wu R, et al. “Motion compensation for UAV SAR based on raw radar data”. IEEE Transactions on Geoscience and Remote Sensing, 2009, 47(8): 2870-2883.

[7] Sze L T, Cheaw W G, Ahmad Z A, et al. “High resolution DEM generation using small drone for interferometry SAR”. Space Science and Communication (IconSpace), 2015 International Conference on. IEEE, 2015: 366-369.

[8] Magnard C, Frey O, Rüegg M, et al. “Improved airborne SAR data processing by blockwise focusing, mosaicking and geocoding”. Synthetic Aperture Radar (EUSAR), 2008 7th European Conference on. VDE, 2008: 1-4.

[9] Li C J, Ling H. “Synthetic aperture radar imaging using a small consumer drone”. Antennas and Propagation & USNC/URSI National Radio Science Meeting, 2015 IEEE International Symposium on. IEEE, 2015: 685-686.

[10] Abidin Z, Munir A. “Development of FMCW SAR on L-band frequency for UAV payload”. Telecommunication Systems Services and Applications (TSSA), 2016 10th International Conference on. IEEE, 2016: 1-5.

[11] Bamler R. “A comparison of range-Doppler and wavenumber domain SAR focusing algorithms”. IEEE Transactions on Geoscience and Remote Sensing, 1992, 30(4): 706-713.